J Mater Sci (2009) 44:3344–3348
DOI 10.1007/s10853-009-3301-6

Fabrication and characterization of novel bowknot-like CeO_2 crystallites and applications for Methyl-orange Sensors

DongEn Zhang · Wei Wu · XinJiang Ni · XiaoYan Cao · XiaoBo Zhang · XingYou Xu · ShanZhong Li · GuiQuan Han · Ailing Ying · ZhiWei Tong

Received: 28 November 2008 / Accepted: 26 January 2009 / Published online: 21 April 2009

Abstract Bowknot-like CeO_2 bundles crystals were successfully prepared from a single precursor via a thermal decomposition route. The precursor was synthesized by a hydrothermal reaction using $Ce(NO_3)_3 \cdot 6H_2O$ with $CO(NH_2)_2$ at 150 °C in a water-glycerol complex solution. Glycerol plays a very important role for the formation of precursor bowknot-like structures. The morphology of the precursor was maintained during the heating process. The optical absorption spectrum indicates that the CeO_2 dendrites have a direct band gap of 3.42 eV, which is mostly larger than values of bulk powders due to the quantum size effect. The electrochemical characters of the CeO_2 bundles structures are studied by their investigation of cyclic voltammetry (CV). It was found that the CeO_2 bundles can greatly improve the electron transfer ability.

D. Zhang · X. Ni · X. Cao · X. Zhang · X. Xu · S. Li · G. Han · A. Ying · Z. Tong
Department of Chemical Engineering, Huaihai Institute of Technology, Lianyungang 222005, People's Republic of China

D. Zhang (✉) · Z. Tong (✉)
SORST, Japan Science and Technology Agency (JST), Kawaguchi-shi, Saitama, Japan
e-mail: zdewxm@yahoo.com.cn

Z. Tong
e-mail: tong@hhit.edu.cn

W. Wu
Department of Electronics Engineering, Southeast University, Nanjing 210018, People's Republic of China

Introduction

As a typical kind of rare earth oxide, ceria has been the subject of intense interest because of its unique properties, including oxygen storage capacity [1] and oxygen ion conductivity [2, 3]. Because of these characteristics, ceria has been widely used for as a promoter in the three-way catalysts for the elimination of toxic auto-exhaust gases [1, 4, 5], as oxygen sensors [6, 7] and as solid electrolytes in the solid oxide fuel cells utilizing their oxygen storage capacity [8–10]; as absorbents for fluoride ion or arsenicbased compounds; and as substances to filter out ultraviolet rays [11]. Cerium oxide also has optical properties, high thermal stability, and electrical conductivity and diffusivity. Previous research has proved that nano/micro-crystalline CeO_2 has superior properties compared with its bulk counterparts [12]. For example, hierarchically mesostructured ceria exhibits a photovoltaic response, while normal ceria does not show this response [13]. Thus, it is urgent to design functional ceria materials with certain size and shape by simple morphology controllable routes. In the past few years, the synthesis of some novel CeO_2 structures, including nanorods [14–16], nanowires [17–21], nanotubes [22, 23], nanocubes [24], microplates [25], and other morphological structures [26–31] have been reported by chemical scientists. In this paper, bowknot-like CeO_2 structures were fabricated by the thermal treatment of the cerium carbonate hydroxide precursor which was synthesized by a hydrothermal reaction using $Ce(NO_3)_3 \cdot 6H_2O$ with $CO(NH_2)_2$ at 150 °C in a water-glycerol (complex solution). It was found that the CeO_2 bundles modified gold electrode was prepared and used to catalysis oxidation of methyl orange in the solution. The results show that the CeO_2 bundles exhibit excellent sensing performance towards methyl orange, which provide a new application of CeO_2 dendrites.

Experimental details

All the reagents are of analytical purity grade and have been received from commercial sources. In a typical synthesis, 10 mL glycerol were added into 30 mL aqueous solution of 0.01 M $Ce(NO_3)_3$ under stirring. Then 0.3 g urea was added. The whole mixture was stirred for another 30 min to obtain a homogeneous solution and subsequently transferred into a 50 mL autoclave. The autoclave was maintained at 150 °C for 12 h and then allowed to cool to room temperature by cold-water. Then, white-colored precipitate was centrifuged, washed with absolute alcohol and distilled water, and dried at 80 °C under vacuum. Finally, for CeO_2 particles were obtained by calcining the precipitate at 500 °C for 4 h accompanied by a color change from white to slight yellow.

X-ray powder difffraction (XRD) patterns were determined using a Philips X'Pert PRO SUPER X-ray diffractometer equipped with graphite-monochromatized Cu Ka radiation ($\lambda = 1.5418$ Å). Field emission scanning electron microscopy (FESEM) images were taken with a JEOL JSM6700F scanning electron microscope. Optical absorption spectrum was recorded on a Shimadzu UV-2401PC UV-vis recording spectrophotometer.

Results and discussion

Figure 1 presents the typical XRD pattern of as-prepared $Ce(OH)CO_3$ samples. All the peaks could be indexed to the hexagonal phase of cerium carbonate hydroxide (JCPDS Data File # 32-0189). The strong and sharp reflection peaks suggest that the as-prepared products are well crystallized.

The TGA curve of the precursor is shown in Fig. 2. There are two weight loss steps at the temperature ranges

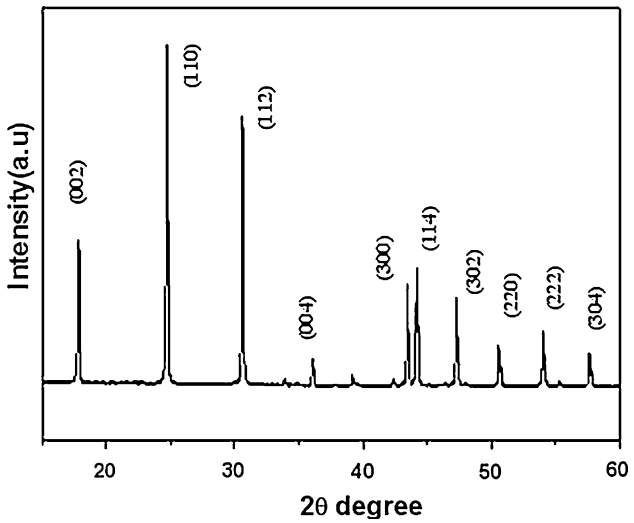

Fig. 1 XRD pattern of the $Ce(OH)CO_3$ precursor

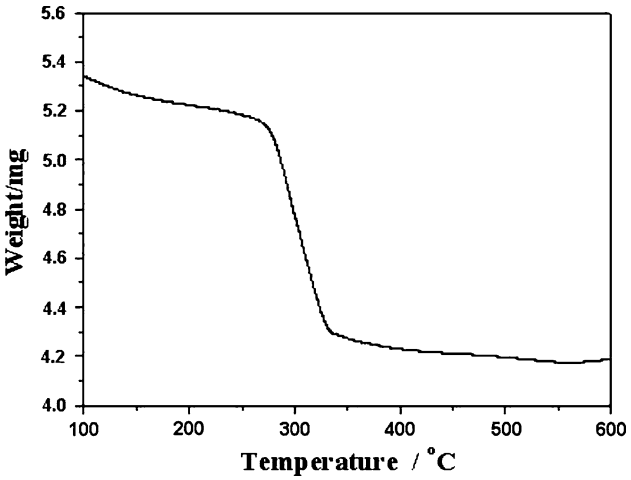

Fig. 2 TG curve of the precursor

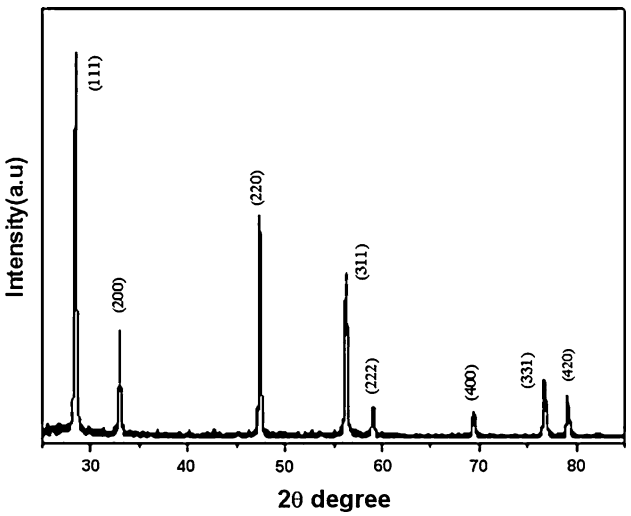

Fig. 3 XRD pattern of the CeO_2 sample

30–275 and 275–340 °C. The first weight loss is mainly attributed to the evaporation of H_2O, whereas the second one may be ascribed to the decomposition of the precursor. The weight-loss process ceases at 340 °C, and the stable residue can be reasonably ascribed to CeO_2.

After the calcination of the obtained precursor at 500 °C in air according to the TGA data, the precursor was converted into CeO_2. Figure 3 presents the typical XRD pattern of as-prepared calcined samples. All the peaks could be indexed to the cubic phase of ceria with fluorite structure (JCPDS Data File # 43-1002). No impurity peaks are observed, indicating the high purity of the final products. The strong and sharp reflection peaks suggest that the as-prepared products are well crystallized.

The morphology and size of as synthesized products were observed by a JEOL JSM6700F scanning electron microscope. Figure 4 shows typical Field emission

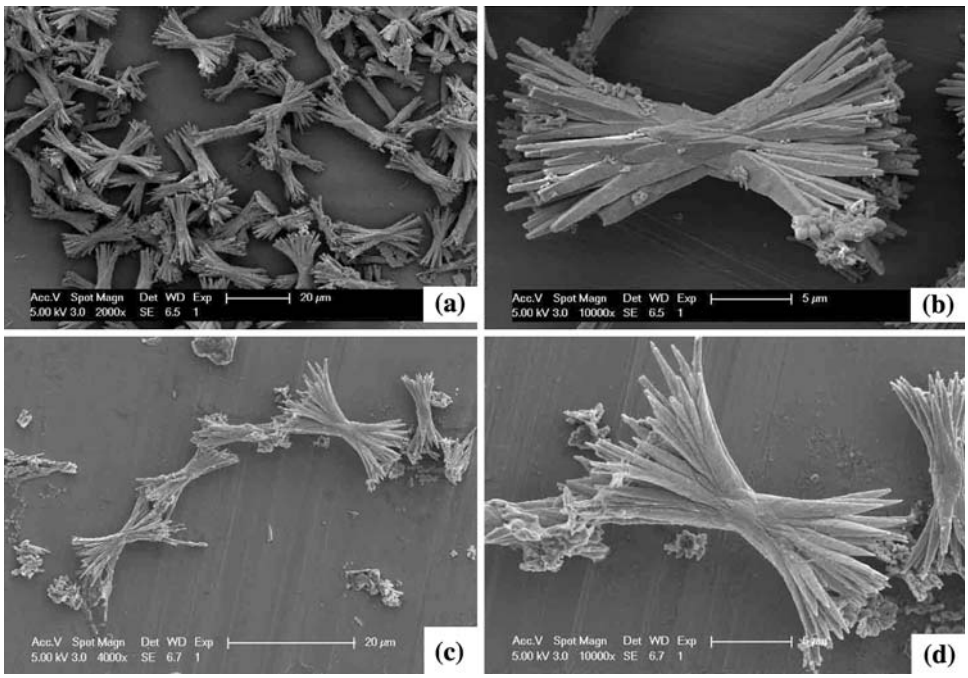

Fig. 4 FESEM images of $Ce(OH)CO_3$ precursor and CeO_2 samples: **a** low magnification of $Ce(OH)CO_3$ precursor; **b** high magnification of $Ce(OH)CO_3$ precursor; **c** low magnification of CeO_2 samples; **d** high magnification of CeO_2 samples

scanning electron microscopy (FESEM) images of $CeOHCO_3$ precursor and CeO_2 samples. The overall morphology of the $CeOHCO_3$ precursor (Fig. 4a) indicates that there exist great deals of uniform bowknot-like bundles and this indicates the high yield and good uniformity achieved with this approach. The overview morphology of individual structure (Fig. 4b) shows bowknot-like bundles with their two ends fanning out while the middle part tying together. The bowknot-like structure is different from the structure of "bunch of nanorods grown from the same nucleus" which forms as many highly aligned individual nanorods growing from one central point toward outside to form straw-bundle-like architectures. After long-period ultrasonic treatment, the bowknot-like $CeOHCO_3$ precursor microstructures were not destroyed, indicating the nanostructures were not due to aggregation. It is well known that $CeOHCO_3$ can be formed by a simple solution process using urea as the precipitant and the heat treatment process does not ruin the morphology of the products [3, 25, 32]. So, the glycerol plays an important role in the formation of $Ce(OH)CO_3$ bowknot-like structures. With regard to the effect of additives on morphology and size of the crystal, there has not yet been an adequate mechanism to account for except the adsorption mechanism that seems to be more reasonable. It is supposed that the bowknot-like structure is obtained through a seed-mediated growth in the presence of glycerol. Glycerol is adsorbed selectively on the different planes of $Ce(OH)CO_3$ seeds, helps lower the surface tension and results in the different growth rates of different planes to form the bowknot-like structures. After $Ce(OH)CO_3$ bowknot-like structures are calcined in air at 500 °C for 6 h, uniform bowknot-like of CeO_2 crystallites are formed. As shown in Fig. 4c and d, FESEM images reveal that the bowknot-like shape of $Ce(OH)CO_3$ was sustained after thermal decomposition-oxidation to CeO_2. Thus-prepared structures were very stable, and even long-time ultrasonication of 20 min could not break them into discrete platelets, suggesting that the bowknot-like were integrative.

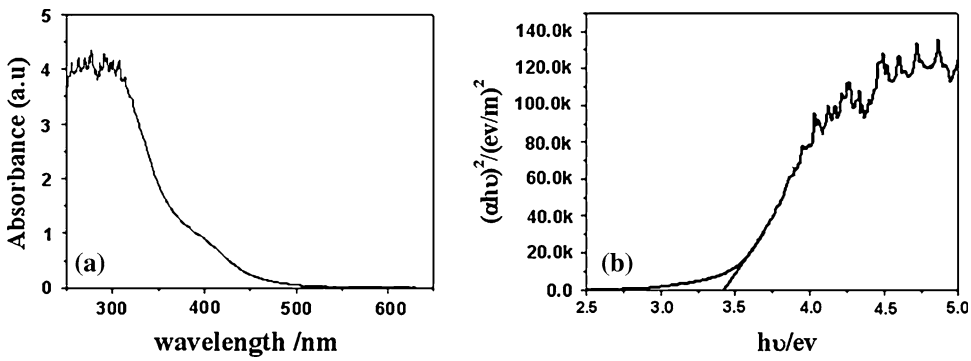

Fig. 5 Optical absorption spectrum and $(\alpha hv)2 \sim hv$ curve for the CeO_2 samples

The UV-visible absorption spectrum of the sample is shown in Fig. 5. It shows that the absorption edge obviously shifts toward shorter wavelength, i.e., blue shift. An estimate of the optical band gap, Eg, can be determined by the following equation for a semiconductor: $(\alpha h\upsilon)n = B(h\upsilon - Eg)$, where $h\upsilon$ is the photo energy, α is the absorption coefficient, B is a constant relative to the material, and n is either 2 for a direct transition or 1/2 for an indirect transition. The $(\alpha h\upsilon)^2 \sim h\upsilon$ curve for the samples is shown in Fig. 5b; it reveals that the band gap of the sample is about 3.41 eV, which is mostly larger than the values of bulk powders (3.19 eV) because of the quantum size effect [33].

Figure 6 exhibited the electrochemical response of methyl orange at the bundles modified electrode, and then cyclic voltammograms at 50 mV s^{-1} of the modified electrode. Under the same experimental conditions, there was almost no obvious redox peak of methyl orange at the bare gold electrode (Fig. 6, curve a). However, it can be seen that the oxidation peak potential of methyl orange at bundle-modified electrode (Fig. 6, curve b) appeared compared with that at a bare gold electrode. Above all, the oxidation peak potential of methyl orange at the modified electrode moved to the negative direction and the peak current for the same amount of methyl orange became large. All these appearance means, the electrochemical response of methyl orange on CeO_2 bundle-modified electrode is better than that on bare electrode. The above phenomena imply that the CeO_2 bundles can greatly improve the electron transfer ability, which may be a direct result of the large surface of the trigons structure. This suggested that the electrocatalytic activity of the modified electrode could be applied to the electrolysis of catalysis oxidation of methyl orange.

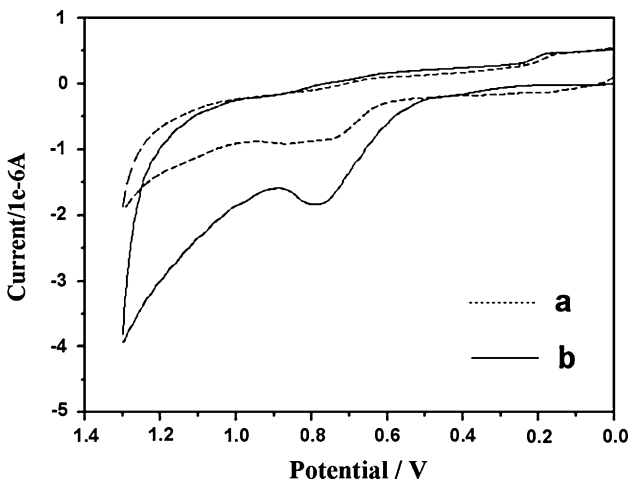

Fig. 6 CV performances of 100. 0 mg/L methyl orange on different electrode at a scan rate of 50 mV s-1: (a) bare; (b) trigons-modified GC electrodes

Conclusion

In summary, we have successfully synthesized bowknot-like CeO_2 structures from a single precursor by a thermal decomposition in a water-glycerol complex solution. Glycerol plays a very important role for the formation of precursor bowknot-like structures. The morphology of the precursor was maintained during the heating process. The optical absorption spectrum indicates that the CeO_2 dendrites have a direct band gap of 3.42 eV, which is mostly larger than the values of bulk powders due to the quantum size effect. The electrochemical response of the as-prepared bundles samples on methyl orange is also investigated. The as-prepared CeO_2 bundles exhibit excellent sensing performance toward methyl orange.

Acknowledgement This work was supported by a Grant-in-aid for Scientific Research from the Japan Society for the Promotion of Science (JSPS), the CREST program of the Japan Science and Technology Agency (JST), the National Natural Science Foundation of China (No. 50873042), the Natural Science Foundation of Jiangsu Province (No. 07KJA15011) and the Scientific Research Program of HuaiHai Institute of Technology (KQ08023, Z2008018). We are grateful to young and middle-aged academic leaders of "Blue and Green Blue Project" of the universities and colleges in Jiangsu Province. We are also grateful to the electron microscope and X-ray diffraction facilities of University of Science & Technology of China for assistance in XRD and SEM measurement.

References

1. Trovarelli A (1996) Catal Rev Sci Eng 38:439
2. Inaba H, Tagawa H (1996) Solid State Ion 83:1
3. Zhong LS, Hu JS, Cao AM, Liu Q, Song WG, Wan LJ (2007) Chem Mater 19:1648
4. Lunderg M, Skaerman B, Cesar F, Wallenberg LR (2002) Micropor Mesopor Mater 54:97
5. Laha SC, Ryoo R (2003) Chem Commun 17:2138
6. Beie HJ, Gnöich A (1991) Sensors Actuators B 4:393
7. Jasinski P, Suzuki T, Anderson HU (2003) Sensors Actuators B 95:73
8. Steele BCH (2000) Solid State Ion 129:95
9. Nair JP, Wachtel E, Lubomirsky I, Fleig J, Maier J (2003) Adv Mater 15:2077
10. Inaba H, Tagawa H (1996) Solid State Ion 83:1
11. Qi RJ, Zhu YJ, Cheng GF, Huang YH (2005) Nanotechnology 16:2502
12. Zhou F, Zhao XM, Xu H, Yuan CG (2007) J Phys Chem C 111:1651
13. Carrettin S, Concepcion P, Corma A, Nieto JML, Puntes VF (2004) Angew Chem Int Ed 43:2538
14. Kuiry SC, Patil SD, Deshpande S, Seal S (2005) J Phys Chem B 109:6936
15. Mai HX, Sun LD, Zhang YW, Si R, Feng W, Zhang HP, Liu HC (2005) J Phys Chem B 109:24380
16. Zhou KB, Wang X, Sun XM, Peng Q, Li YD (2005) J Catal 229:206
17. Wu GS, Xie T, Yuan XY, Cheng BC, Zhang LD (2004) Mater Res Bull 39:1023
18. Yada M, Sakai S, Torikai T, Watari T, Fyruta S, Katsuki H (2004) Adv Mater 16:1222

19. Sun CW, Li H, Wang ZX, Chen LQ, Huang XJ (2004) Chem Lett 133:662
20. Yang R, Guo L (2005) J Mater Sci 40:1305. doi:10.1007/s10853-005-6958-5
21. La RJ, Hu ZA, Li HL, Shang XL, Yang YY (2004) Mater Sci Eng A 368:145
22. Han WQ, Wu LJ, Zhu YM (2005) J Am Chem Soc 127:12814
23. Yang R, Guo L (2004) Chin J Inorg Chem 20:152
24. Yang SW, Gao L (2006) J Am Chem Soc 128:9330
25. Guo ZY, Du FL, Cui ZL (2006) Inorg Chem 45:4167
26. Sun CW, Sun J, Xiao GL, Zhang HR, Qiu XP, Li H, Chen LQ (2006) J Phys Chem B 110:13445
27. Wang ZL, Feng XD (2003) J Phys Chem B 107:13563
28. Laberty-Robert C, Long JW, Lucas EM, Pettigrew KA, Stroud RM (2006) Chem Mater 18:50
29. Huang S, Li L, Van der Biest O, Vleugels J (2005) Solid State Sci 5:539
30. Zhang DE, Ni XM, Zheng HG, Zhang XJ, Song JM (2006) Solid State Sci 8:1920
31. Wu XD, Wu XD, Liang Q, Fan J, Weng D, Xie Z, We SQ (2007) Solid State Sci 9:636
32. Wang SF, Gu F, Li CZ, Cao HM (2007) J Crys Grow 307:386
33. Liao XH, Zhu JM, Zhu JJ, Xu JZ, Chen HY (2001) Chem Commun 10:937